

Drained pore modulus determination using digital rock technology

***Shakil Ahmed**

CSIRO Energy
26 Dick Perry Avenue
Kensington, Perth, WA 6151
Australia
Shakil.Ahmed@csiro.au

Tobias Müller

CSIRO Energy
26 Dick Perry Avenue
Kensington, Perth, WA 6151
Australia
Tobias.Mueller@csiro.au

Mahyar Madadi

Curtin University
26 Dick Perry Avenue
Kensington, Perth, WA 6151
Australia
Mahyar.Madadi@curtin.edu.au

Victor Calo

Curtin University
CSIRO Mineral Resource
Bentley, Perth, WA 6845
Australia
Victor.Calo@csiro.au

SUMMARY

Geomechanics helps us understand the life-cycle of a hydrocarbon reservoir and, in turn, impacts geophysical monitoring programs. A common geomechanical problem is to predict reservoir compaction or zones of abnormal pore pressure. These predictions mostly use simple empirical relations, but recently, the use of rock deformation models based on static poroelasticity are becoming the norm. These models require accurate values for the poroelastic parameters. We present a digital rock workflow to determine these poroelastic parameters which are difficult to extract from well-log or laboratory measurements. The drained pore modulus is determinant in the compaction problem. This modulus represents the ratio of pore volume change to confining pressure when the fluid pressure is constant. In laboratory experiments, bulk volume changes are accurately measured by sensors attached to the outer surface of the rock sample. In contrast, pore volume changes are notoriously difficult to measure because these changes need to quantify the pore boundary deformation. Hence, accurate measures of the drained pore modulus are challenging. We simulate static deformation experiments at the pore-scale utilizing digital rock images. We model an Ottawa F-42 sand pack obtained from X-ray micro-tomographic images. We stack two-dimensional micro-CT images to generate a three-dimensional F-42 sand pack sample. We extract a sub-volume from this sample for numerical simulation. We first segment the cropped sample consists of grains and pore spaces and then use the segmentation to generate a volumetric mesh. We compute the elastic, linear momentum balance in the structural domain (grains) and solve the system using the commercial software package ABAQUS. The network of grains (solid phase) is assumed elastic, isotropic, and homogeneous. We calculate the change in pore volume using a new post-processing algorithm, which allows us to compute the local changes in pore volume due to the applied load. This process yields an accurate drained pore modulus. We then use an alternative estimate of the drained pore modulus. We exploit its relation to the drained bulk modulus and the solid phase bulk modulus (i.e., Biot's coefficient) using the digital rock workflow. Finally, we compare the drained pore modulus values obtained from these two independent analyses and find reasonable agreement.

Key words: Drained pore modulus, Biot coefficient, Digital rock workflow, Poroelasticity.

INTRODUCTION

A standard model for the effective elastic behaviour of porous, fluid-saturated rocks is the theory of linear poroelasticity, which is a macroscopic theory. This means only an average of the textural and compositional complexities at pore-scale enter the poroelastic description. Since the introduction of the poroelasticity theory by Biot (1941), the definition of an effective deformation moduli for the constitutive relations has been sought (Biot and Willis, 1957; Makhnenko and Labuz, 2016; and Cheng, 2016 for an overview). We use volume averaging of the pore-scale equations to define this parameter (Sahay et al., 2001; Sahay, 2013; Müller and Sahay, 2013; Müller and Sahay, 2016a), which describes the effects of pore-scale heterogeneities.

In geomechanical reservoir analysis the Biot coefficient allows us to estimate the reservoir stress path (Altmann et al., 2010). The Biot coefficient represents the fluid volume change induced by the bulk volume change in drained conditions, which is difficult to measure in the laboratory. An alternative definition of the coefficient is as the effective pressure coefficient for the bulk that is measured in constant bulk volume tests (e.g. Omdal et al., 2009). However, this interpretation is not correct in micro-inhomogeneous rocks (Müller and Sahay, 2016b). The drained pore modulus is relevant in some geotechnical applications such as reserve estimation (e.g. Schutjens and Heidug, 2012; De Oliveira et al., 2016). The drained modulus measures the change of pore volume as the confining pressure increases while the fluid pressure is constant. This drained coefficient is as difficult to measure in the laboratory as the Biot coefficient.

Given these problems, we define new avenues to estimate the Biot coefficient and the drained pore modulus using digital rock technology (DRT). DRT technology uses 3D pore-scale images of rocks (i.e., the geometry of the pore-scale features is known and only limited by the resolution of the imaging process) in conjunction with numerical solvers for the pore-scale governing equations. Specifically, we improve the understanding of the drained pore modulus through digitized rock simulations. We numerically simulate static deformation experiments at the pore-scale utilizing digitized rock images of sandstone. From the pore-scale simulations we infer the macroscopic deformation moduli by volume-averaging. We interpret these moduli in the framework of a generalized poroelasticity framework that accounts for micro-inhomogeneities in a generic way (Müller and Sahay, 2016a).

MODELING FRAMEWORK FOR MICRO-INHOMOGENEOUS ROCKS

Constitutive equations of linear poroelasticity and the porosity perturbation equation

We consider an isotropic poroelastic solid and restrict the analysis to volumetric changes only. Then, there are the following kinematic variables of interest: The bulk volumetric strain (ε) and the increment of fluid content (ζ) according to Biot's (1941) consolidation theory, where we adopt the notation of Wang (2000). In addition, since pore boundaries move during deformation (Figure 1) the proportion of solid to fluid volume changes and amounts to a change of porosity is $(\eta - \eta_0)$. Here η is the porosity at the current state of deformation and η_0 is the porosity at the reference (undeformed) state. While the change of porosity does not appear explicitly in Biot's theory, Sahay (2013) has shown that there is always an underpinning porosity equation. These three kinematic variables can be changed by a combination of the fluid pressure (p^f) and the confining pressure (p^c). The latter is equal to the total pressure

$$p^c = \eta_0 p^f + (1 - \eta_0) p^s . \quad (1)$$

Herein $(1 - \eta_0) p^s$ represents the macroscopic pressure of the solid phase which is related to the macroscopic solid stress tensor τ_{jk}^s appearing in Biot's constitutive equations (Biot and Willis, 1957) via $-(1 - \eta_0) p^s = 1/3 \tau_{kk}^s$. For macroscopically homogeneous porous material and in the realm of equilibrium thermodynamics the constitutive poroelastic equations are (Müller and Sahay, 2016a, their equations 16-18)

$$-p^c = K_0 \varepsilon - \alpha^* p^f \quad (2)$$

$$-\frac{1}{M^*} p^f = \alpha \varepsilon - \zeta \quad (3)$$

and the underpinning porosity perturbation equation is

$$\eta - \eta_0 = -\frac{\alpha - \eta_0}{K_0} \left(p^c - (\eta_0 + (1 - \eta_0) n) p^f \right) . \quad (4)$$

In equation (2) K_0 is the drained frame bulk modulus and

$$\frac{1}{M^*} = \frac{\eta_0}{K_f} + \frac{\alpha^* - \eta_0}{K_s} \quad (5)$$

is the fluid storage coefficient. The bulk moduli of the solid and fluid phase are K_s and K_f , respectively. The porosity perturbation equation entails the parameter n as a macroscopic measure for micro-inhomogeneity and differs from the Biot porosity equation in that the porosity change is not simply determined by the difference pressure (Sahay, 2013). The constitutive equations (2) and (3) also differ from the Biot constitutive equations in that the Biot coefficient (α) and the effective pressure coefficient for the bulk volume (α^*) are taken as distinct quantities (Müller and Sahay, 2016b) as well as the fluid storage coefficient involves the effective pressure coefficient for the bulk volume. These constitutive equations are based on the volume averaging approach of poroelasticity developed in Sahay et al. (2001); see also Sahay (2013) for further details.

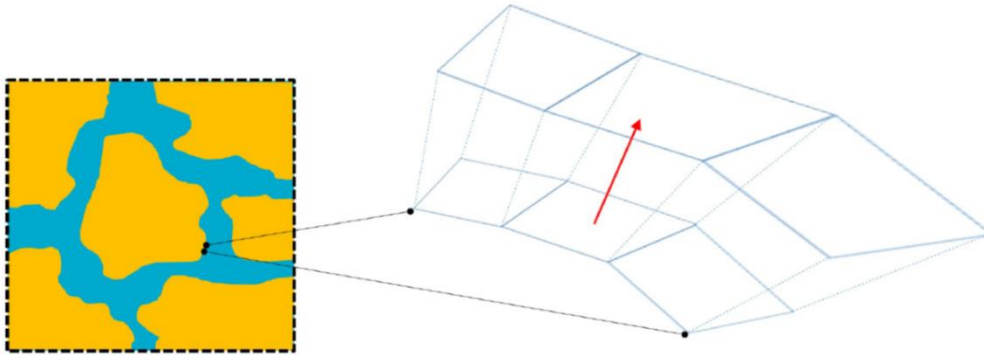


Figure 1. Sketch of a fluid-saturated porous rock at pore scale (left) and oriented surface element with normal of the pore-interface before and after (infinitesimal) deformation (right). At macroscale, there is a porosity change due to displacement in direction of the surface normal.

Moduli relevant for drained rock characterization and their micromechanical representation

In this paper we focus on drained rock moduli and their interrelations. Drained behaviour refers to a state where the fluid pressure is constant. From a micromechanical point of view, the bulk volume (V_b) is the sum of the volume of the solid phase (V_s) and the pore volume (V_p), $V_b = V_s + V_p$ and the porosity is given by the ratio $\eta = V_p/V_b$. Then, to first order, pore volume changes are composed of bulk volume changes and a change in porosity,

$$dV_p = \eta_0 dV_b + V_{b0} d\eta, \quad (6)$$

where the subscript 0 refers to the unperturbed (before deformation) value. Thus, in a drained experiment (setting the fluid pressure to zero) this pore volume change becomes

$$\left. \frac{\partial V_p}{\partial p^c} \right|_{p^f=0} = \eta_0 \left. \frac{\partial V_b}{\partial p^c} \right|_{p^f=0} + V_{b0} \left. \frac{\partial \eta}{\partial p^c} \right|_{p^f=0} . \quad (7)$$

Multiplying by $-1/V_{p0}$ the left-hand side is by definition the drained pore modulus

$$-\frac{1}{V_{p0}} \left. \frac{\partial V_p}{\partial p^c} \right|_{p^f=0} \equiv \frac{1}{K_p} . \quad (8)$$

It is a measure of how much the pore volume changes in response to a change in confining pressure. The first term on the right-hand side in equation 7 is the drained bulk modulus

$$-\frac{1}{V_{b0}} \left. \frac{\partial V_b}{\partial p^c} \right|_{p^f=0} \equiv \frac{1}{K_0} \quad (9)$$

and is routinely measured in pressure cell experiments. The second term on the right-hand side in equation 7 can be evaluated from the porosity perturbation equation (4)

$$\left. \frac{\partial \eta}{\partial p^c} \right|_{p^f=0} = -\frac{\alpha - \eta_0}{K_0} . \quad (10)$$

The Biot coefficient is defined through the constitutive equation (3)

$$\left. \frac{\partial \zeta}{\partial \varepsilon} \right|_{p^f=0} \equiv \alpha . \quad (11)$$

This equation implies that a change of the increment of fluid content due to a change in the bulk volume at zero fluid pressure can only depend on the mechanical properties of the porous frame and on the solid grains that constitute this frame. The bulk modulus associated with the porous frame is the drained frame bulk modulus K_0 . The bulk modulus of the solid-phase K_s could be obtained by applying the same load on the inner and outer surfaces of the porous frame. It is thus determined in hydrostatic compression experiment wherein the change of the solid volume V_s is monitored. Thus

$$-\frac{1}{V_{s0}} \left. \frac{\partial V_s}{\partial p^f} \right|_{p^f=p^c} \equiv \frac{1}{K_s} . \quad (12)$$

This stipulates that the Biot coefficient is expressed in terms of the drained and solid phase bulk moduli

$$\alpha = 1 - \frac{K_0}{K_s} . \quad (13)$$

Substituting the last expression for α into equation (10) and the resulting expression into equation (7) and noting the definitions of the drained bulk and pore modulus yields to the interrelation

$$\frac{\eta_0}{K_p} = \frac{1}{K_0} - \frac{1}{K_s} . \quad (14)$$

Equations (13) and (14) allow us to determine the Biot coefficient and the drained pore modulus for a given porosity, drained bulk modulus and the solid phase bulk modulus. We note that equation (14) is difficult to verify in laboratory experiments because the pore and solid phase bulk modulus would require to measure the changes in pore and solid volume (while typically the bulk volume changes are monitored only). In the following we estimate K_p in two different ways, first from the definition of K_p for a digital rock sample using equation (8) and then by estimating K_0 and K_s (with known porosity) using equation (14). We then compare and discuss our estimated values of K_p obtained from two independent analyses.

DIGITAL ROCK WORKFLOW

General Workflow

Digital rock technology (DRT) is an increasingly accepted and effective tool in the oil and gas industries for investigating petro-physical and elastic properties of rock material. Two types of workflows are available in DRT. In the first one, important micro-structural information is obtained by analysing micro CT scan images with the help of image processing software. The second workflow consists of multi-physics modelling where 2D micro CT scan images are stacked to create a 3D digital sample replicating the real micro-structure. The images are then segmented into separable pore and grain spaces. Pore spaces are used to calculate the petro-physical properties like permeability, porosity, relative permeability and residual fluid distribution within the rock sample. The framework of grains is subjected to stress and strain and effective elastic properties like grain, bulk and pore modulus are calculated. This paper describes the estimation of drained pore modulus of a real rock sample in two different methods using the DRT and an extension work of Ahmed et al. (2017).

The 3D digitized rock sample and properties of the network of grains

The numerical workflow includes a digitized rock sample (Ottawa F-42 sand pack with porosity $\eta_0=0.33$) obtained from X-ray micro-computer tomographic (CT) images. 2D micro-CT image slices are stacked together to generate the 3D F-42 sand pack sample of size 541x431x396 voxels with a voxel size of 5.78 μ m. A small sub-volume consisting of grains and pore spaces of size 100x100x100

voxels is extracted from this sample and is used for analysis. The grains are segmented from pore spaces (Figure 2a) and are used to generate a volume mesh (Figure 2b). The mesh consists of tetrahedral elements. The total number of elements is 353192.

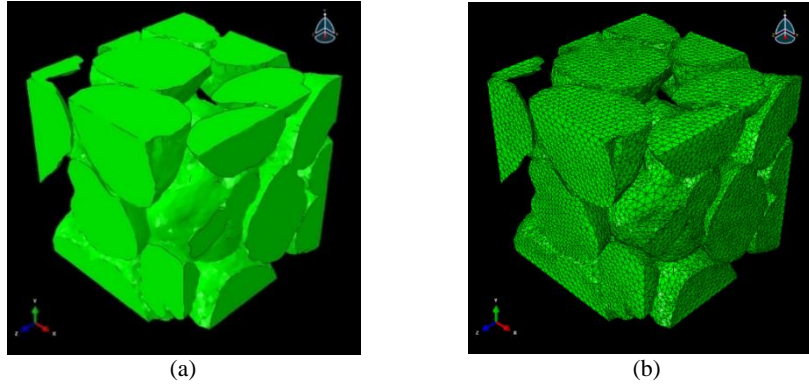


Figure 2. (a) Network of grains constituting the solid phase and (b) volume mesh used for grain analysis.

The governing equation for the structural domain (grains) is the linear momentum conservation equation. It is solved on structural elements using the commercial software package ABAQUS. The grain material is assumed to be linear elastic, isotropic and homogeneous with a density of 2650 kg/m^3 and a Young's modulus and Poisson's ratio of 94 GPa and 0.075 (resembling quartz with bulk and shear modulus $K = 37 \text{ GPa}$ and $\mu = 44 \text{ GPa}$, see Mavko et al. 2008), respectively.

Calculation of the drained bulk and pore moduli and boundary conditions

To directly estimate the K_p we use its micromechanical definition (equation 8) and use the volume mesh in each loading step. The displacement vectors and solid volume changes can be extracted in each loading step. To do so, we can extract the Cartesian coordinate of each node in each loading step from the ABAQUS simulation. Then we calculate the displacement of each single node with respect to the previous loading step. To identify which elements constitute the interior surface (the pore interface), we use summation of number of neighbour elements for each element to extract inner-pore solid nodes, as well as elements. This neighbourhood numbers are minimum for the smooth inner-boundaries and it is maximum if the solid element is surrounded by solid elements. As the element is a solid tetrahedron shape with three polyhedron edge vectors as \vec{a} , \vec{b} , and \vec{c} then the elements volume (v_s) is calculated from

$$v_s = \frac{1}{6} |\vec{a} \cdot (\vec{b} \times \vec{c})|. \quad (15)$$

Then the pore volume for each loading step is $V_p = V_{po} - \sum \delta v_s$, where the summation extends over all elements and over all pervious loading steps. The pore volume change for each loading step is:

$$\Delta V_p = - \sum \delta v_s \quad (16)$$

In accordance with equation (8) we estimate the drained pore modulus from the slope of the pore volume changes with respect to pressure load.

To indirectly estimate K_p we make use of equation (14). This means that we first calculate the solid phase bulk modulus according to its definition (equation 12), for which a uniform, positive traction is applied to all faces of the framework of grains, that is to all external and internal surface elements thereby simulating an all-sided pressure perturbation (pink arrows in Figures 3a). In case of drained bulk modulus, no traction is applied at the internal grain-pore interfaces but at the external surfaces thereby simulating an exterior pressure perturbation (Figures 3b). The pressure is then varied from 1 to 2 MPa and the corresponding volumetric strain is computed. Small pressure values are chosen to make sure that the numerical experiments correspond to linear elastic deformation.

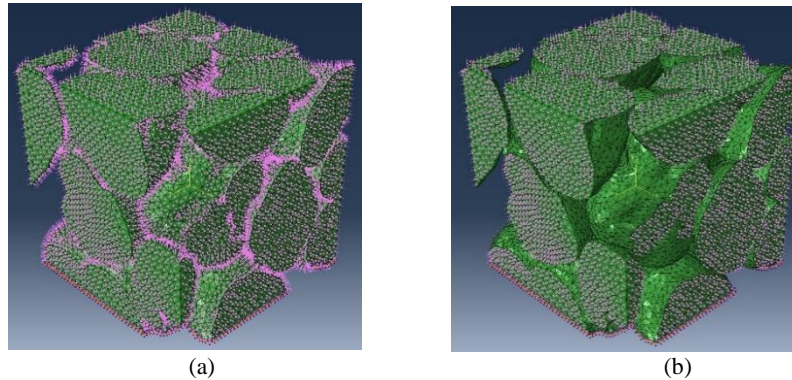


Figure 3. Boundary conditions used for determination of the (a) solid phase bulk modulus via all-sided compression and (b) drained bulk modulus via compression of the outer surfaces.

Numerical results

Figure 4 illustrates the von-Mises stress and volumetric strain distribution of grains during all-sided and external-surface only deformations.

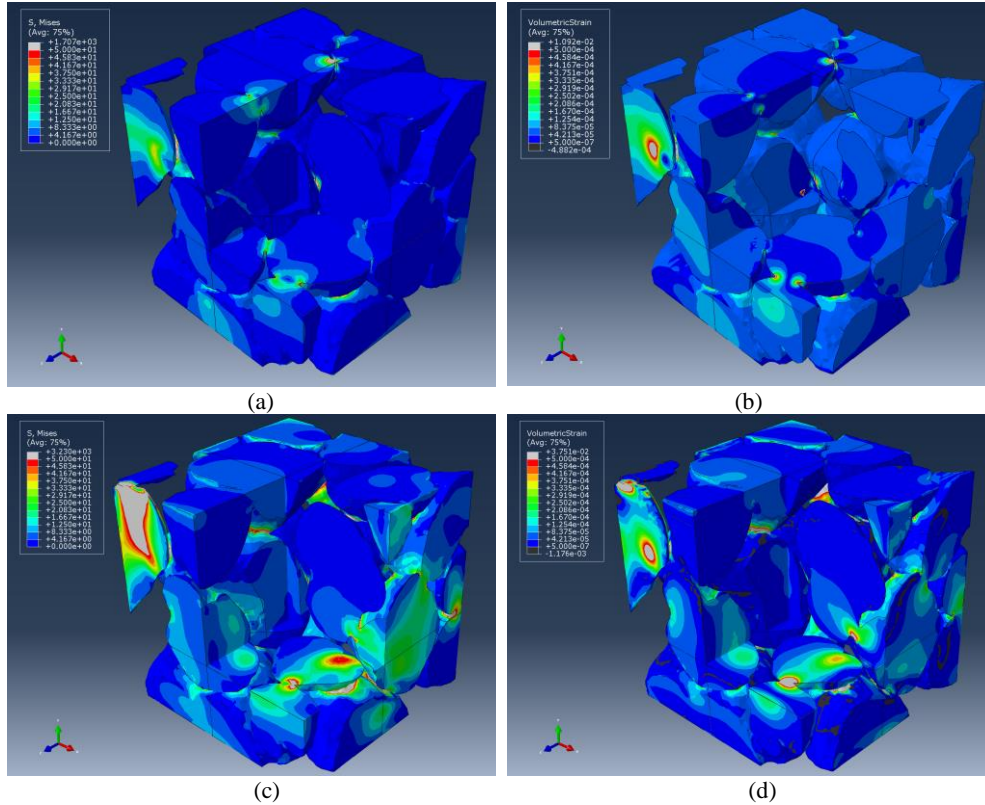


Figure 4. (a) Stress (von Mises stress in MPa) and (b) volumetric strain distribution during all-sided compression. (c) Stress (von Mises stress in MPa) and (d) volumetric strain distribution during compression of the outer surfaces. Note that in both cases the stress and volumetric strain field is not homogeneous. Both stress and volumetric strain concentration are highest in the vicinity of grain contacts.

Volume averaged volumetric strain is calculated and plotted against the pressure confirming the linear deformation case (Figure 5). As shown in the equation (8), we can calculate the pore volume changes in each loading steps. We calculate these changes, and plot them in the Figure 6. This shows that the pore volume changes linearly with the applied pressure. The red curve is best fitted line in the data. The slope of this plot yields to $K_p^{\text{dir}} = 19.02$ GPa.

For the indirect estimating of the drained pore modulus based on equation (14), the solid phase bulk modulus and drained bulk modulus are calculated from the slope of the pressure-volumetric strain relations. We obtain $K_s=38.4$ GPa and $K_0=23.4$ GPa. Substituting these moduli into equation (14) and taking into account that the porosity is $\eta_0=0.33$ we obtain the drained pore modulus $K_p^{\text{ind}}=19.77$ GPa.

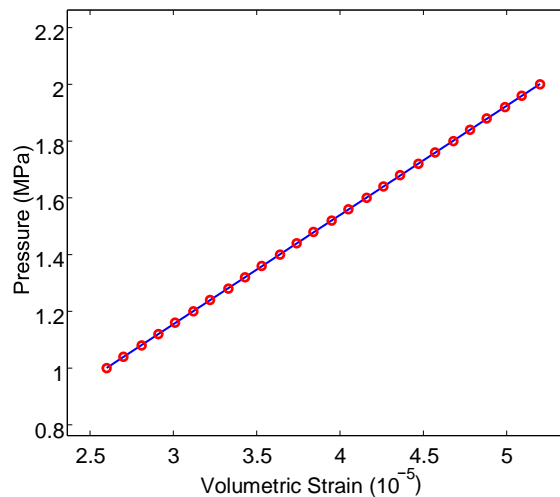


Figure 5. Applied pressure versus computed volumetric strain. The slope determines the bulk modulus.

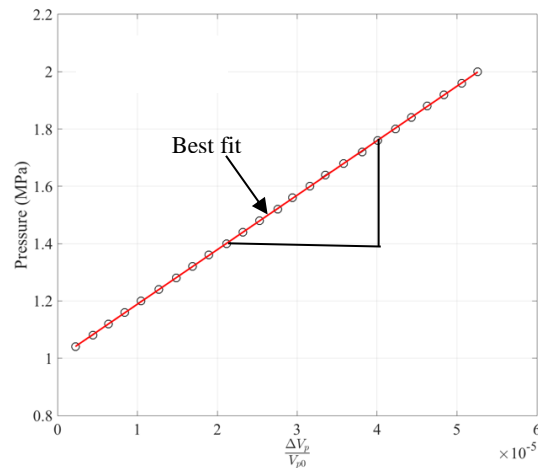


Figure 6. Applied pressure versus the pore volume changes estimated from the deformation of volume during loading. The corresponding drained pore modulus is determined from the slope of best fitted line

DISCUSSION

The direct and indirect estimate of drained pore modulus differ by ~ 0.75 GPa. This difference is considered to be within the range of numerical errors. Our procedure for the direct calculation of K_p is prone to error because here we assume that the local change in pore volume can be approximated by the change of volumetric strain of a tetrahedral element. For the determination of K_0 the bulk volume changes are computed from the displacements of the outer surfaces of the sample. Given that one of this outer surface is fixed in space (to make the ABAQUS simulations feasible) we introduce another error which we only compensate for in an approximate manner. Also the size of tetrahedral elements matters. Finally, another source of error is related to the size of the representative elementary volume (REV) that is needed to make the moduli predictions meaningful at the scale of a typical rock sample used in laboratory investigations. The chosen subsample size is relatively small and we have not verified how much our predictions would change if larger sample sizes were used.

It is interesting to note that De Oliviera et al. (2016) measure the pore volume compressibility for a suite of reservoir sandstones samples. For a sandstone of similar porosity (their Botucatu sandstone sample has porosity 0.3) they report a value of K_p that is significantly smaller (≈ 0.5 GPa) than our numerical estimate. Jalalh (2006) obtains for a friable reservoir sandstone ($\eta_0 = 0.3$) the value $K_p = 2.3$ GPa at high confining pressure (see Figure 9 in Jalalh, 2006). These lower values of K_p found from laboratory measurements could indicate that our digital rock simulation overestimates the drained pore modulus. This is perhaps not unexpected since digital rock simulations tend to overestimate the drained frame modulus and hence the drained pore modulus when applied to images from consolidated rock samples. The reason is that grain contacts typically add some compliance to the rock skeleton and therefore reduce the overall stiffness. However, in the sand pack images these compliant grain contact areas are not present and therefore a higher K_p appears plausible.

CONCLUSIONS

We estimate the drained pore modulus, the drained bulk modulus and the modulus of the solid phase for digitized images of a sand pack using numerical simulations. We verify the interrelation among the moduli using poroelasticity theory using an idealized porous rock model and find a reasonable agreement between the simulations. Our results demonstrate that digital rock technology can determine relevant porous medium parameters which are difficult to assess in the laboratory. The comparison with other laboratory measurements for consolidated sandstones of similar porosity indicate the drained pore modulus is too high. The reason for this discrepancy is probably the absence of compliant grain contact areas in the digitized sand pack images.

REFERENCES

- Ahmed, S., Müller, T. M., Liang, J., Tang, G., and Madadi, M., 2017, Macroscopic deformation moduli of porous rock: Insights from digital image pore-scale simulations: 6th Biot conference on poromechanics, July 9-13, 2017, Paris, France.
- Altmann, J., Müller, T. M., Müller, B. I. R., Tingay, M. R. P., and Heidbach, O., 2010, Poroelastic contribution to the reservoir stress path: *International Journal of Rock Mechanics and Mining Science*, 47, 1104–1113,
- Biot, M.A., 1941, General theory for three-dimensional consolidation: *Journal of Applied Physics*, 12, 155-164.
- Biot, M.A., and Willis, D.G., 1957, The elastic coefficients of the theory of consolidation: *Journal of Applied Mechanics*, 24, 594601.
- Cheng, A.H.-D., 2016, *Poroelasticity*: Springer, New York.

- De Oliviera, G.P., Ceia, M.A.R., Missagia, R.M., Archilha, N.L., Figueiredo, L., Santos, V.H., and Lima Neto, I., 2016, Pore volume compressibilities of sandstones and carbonates from Helium porosimetry measurements: *Journal of Petroleum Science and Engineering*, 137, 185-201.
- Jalalh, A.A., 2006, Compressibility of porous rocks: Part I. Measurements of Hungarian reservoir rock samples: *Acta Geophysica*, 54, 319-332.
- Makhnenko, R.Y., and Labuz, J.F., 2016, Elastic and inelastic deformation of fluid saturated rock: *Phil. Trans. R. Soc. A*, 374, 20150422.
- Mavko, G., Dvorkin, J. Mukerji, T., 2008, *Rock Physics Handbook: Tools for Analysis of Porous Media*, Cambridge.
- Müller, T. M., and P. N. Sahay, 2013, Porosity perturbations and poroelastic compressibilities: *Geophysics*, 78, no. 1, A7–A11.
- Müller, T.M., and Sahay, P.N., 2016a, Generalized poroelasticity framework for micro-inhomogeneous rocks: *Geophysical Prospecting*, 64, 1122-1134.
- Müller, T.M., and Sahay, P.N., 2016b, Biot coefficient is distinct from effective pressure coefficient: *Geophysics*, 81, L27-L33.
- Omdal, E., M. Madland, H. Breivik, K. Naess, R. Korsnes, A. Hiorth, and T. Kristiansen, 2009, Experimental investigation of the effective stress coefficient for various high porosity outcrop chalks: Presented at the 43rd US Rock Mechanics Symposium and 4th U.S.-Canada Rock Mechanics Symposium, 1–4.
- Sahay, P. N., Spanos, T. J. T., and de la Cruz, V., 2001, Seismic wave propagation in inhomogeneous and anisotropic porous media: *Geophysical Journal International*, 145, 209–222.
- Sahay, P. N., 2013, Biot constitutive relation and porosity perturbation equation: *Geophysics*, 78, no. 5, L57–L67
- Schutjens, P. and Heidug, W., 2012, On the pore volume compressibility and its application as a petrophysical parameter: 9th Biennial International Conference & Exposition on Petroleum Geophysics, P-512, 1-17.
- Wang, H. F., 2000, *Theory of Linear Poroelasticity*: Princeton University Press, New Jersey.